Physics Letters A 381 (2017) 3884–3892

Contents lists available at ScienceDirect

Physics Letters A

www.elsevier.com/locate/pla

Coupled pendula chains under parametric $\mathcal{PT}$-symmetric driving force

E. Destyl [a], S.P. Nuiro [a], D.E. Pelinovsky [b,c,*], P. Poullet [a]

[a] LAMIA, Université des Antilles, Campus de Fouillole, F-97157 Pointe-à-Pitre, Guadeloupe
[b] Department of Mathematics, McMaster University, Hamilton, Ontario, L8S 4K1, Canada
[c] Department of Applied Mathematics, Nizhny Novgorod State Technical University, 24 Minin street, 603950 Nizhny Novgorod, Russia

ARTICLE INFO

Article history:
Received 26 August 2017
Received in revised form 11 October 2017
Accepted 11 October 2017
Available online 16 October 2017
Communicated by C.R. Doering

Keywords:
Discrete nonlinear Schrödinger equation
$\mathcal{PT}$-symmetry
Stability of zero equilibrium
Dynamics of coupled pendula

ABSTRACT

We consider a chain of coupled pendula pairs, where each pendulum is connected to the nearest neighbors in the longitudinal and transverse directions. The common strings in each pair are modulated periodically by an external force. In the limit of small coupling and near the 1 : 2 parametric resonance, we derive a novel system of coupled $\mathcal{PT}$-symmetric discrete nonlinear Schrödinger equations, which has Hamiltonian symmetry but has no phase invariance. By using the conserved energy, we find the parameter range for the linear and nonlinear stability of the zero equilibrium. Numerical experiments illustrate how destabilization of the zero equilibrium takes place when the stability constraints are not satisfied. The central pendulum excites nearest pendula and this process continues until a dynamical equilibrium is reached where each pendulum in the chain oscillates at a finite amplitude.

1. Introduction

Coupled pendula models are fundamental in the theoretical physics as they can be used for modelling of many interesting physical phenomena, ranging from DNA dynamics to crystal structure of solid states [7]. Synchronization of coupled pendula and destabilization of their dynamics due to various parametric forces have been studied in much detail [17]. A recent progress towards analytical studies of such models complemented with robust numerical methods was achieved by reducing the second-order Newton's equations to the amplitude equations of the discrete nonlinear Schrödinger (dNLS) type [11].

Parametric resonance in a chain of coupled pendula due to a horizontally shaken pendulum chain was studied experimentally and analytically in [10,13,22]. Numerical approximations were employed in these papers in order to characterize dynamics of coupled pendula in the presence of bistability. Another example of recent studies of parametrically driven chains of coupled pendula can be found in [20,21], where existence and stability of discrete breathers have been addressed numerically.

It was realized in [3,4] that the parametrically driven coupled pendula can be analytically studied by using Hamiltonian systems of the dNLS type in the presence of gains and losses. Such systems are simultaneously Hamiltonian and $\mathcal{PT}$-symmetric, where the parity ($\mathcal{P}$) and time-reversal ($\mathcal{T}$) symmetries were used first to characterize the non-Hermitian Hamiltonians [5] and have now been widely observed in many physical experiments [6,19]. In the recent study [8,9], the presence of Hamiltonian formulation for a class of $\mathcal{PT}$-symmetric dNLS equations was used to employ methods of Hamiltonian dynamics in order to characterize stability and long-time dynamics of breathers in the parametrically driven chains of coupled pendula.

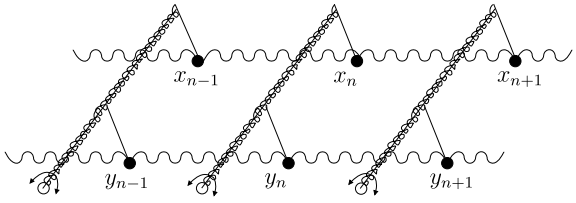

Fig. 1. A graphical illustration for the chain of coupled pendula connected by torsional springs, where each pair is hung on a common horizontal string.

The main goal of this work is to derive and to study a novel model of the coupled $\mathcal{PT}$-symmetric dNLS equations which describes parametrically driven chains of the coupled pendula pairs connected to the nearest neighbors in the longitudinal and transverse directions. Fig. 1 gives a graphical illustration of the coupled pendula chain. Compared to the recent work in [8], we consider different couplings between the two pendula in a pair. This coupling describes interactions between the two pendula connected to each other by a common horizontal string.

* Corresponding author.
E-mail address: dmpeli@math.mcmaster.ca (D.E. Pelinovsky).

https://doi.org/10.1016/j.physleta.2017.10.021
0375-9601/

The new feature of the coupled $\mathcal{PT}$-symmetric dNLS model derived here is that the model is Hamiltonian but not phase-invariant, compared to the previously considered class of $\mathcal{PT}$-symmetric models [4,8]. As a result, the model admits only one integral of motion, given by the conserved energy of the system. Nevertheless, existence of this integral of motion allows us to characterize analytically the linear and nonlinear stability of the zero equilibrium in the system. In the stability region, the chain of coupled pendula perform stable oscillations which are determined by the initial deviations of the pendula from the equilibrium.

In order to characterize the destabilization of the coupled pendula chain in the instability region, we employ numerical experiments. We will show numerically that the central pendulum excites nearest pendula and this process continues until a dynamical equilibrium is reached where each pendulum in the chain oscillates at a finite amplitude. While the ℓ^∞ norm of the oscillation amplitudes remains finite at the dynamical equilibrium, we show numerically that the ℓ^2 norm of the oscillation amplitudes diverges in an unbounded chain of coupled pendula as the time goes to infinity. The question of whether the oscillation amplitudes can diverge to infinity in the $\mathcal{PT}$-symmetric dNLS models have been a subject of active research, see, e.g., [12,15,16,18].

Note that divergence of the ℓ^2 norm of the oscillation amplitudes does not contradict the energy conservation as the conserved energy may not be coercive with respect to the oscillation amplitudes. Depending on the parameters of the model, we find conditions when the conserved energy is coercive and this guarantees that the ℓ^2 norm of the oscillation amplitudes does not grow in such parameter configurations. However, coercivity is lost for the other parameter configurations, for which we observe unbounded growth of the ℓ^2 norm of the oscillation amplitudes with bounded ℓ^∞ norm of the oscillation amplitudes.

The paper is organized as follows. Section 2 describes Newton's equations of motion for the chain of coupled pendula and the derivation of the $\mathcal{PT}$-symmetric dNLS model. Section 3 addresses linear stability of the zero equilibrium. Section 4 contains the main analytical results on nonlinear stability of the coupled pendula. Section 5 reports outcomes of the numerical experiments. Section 6 concludes the paper.

We use the following standard notations. For a sequence $\{a_n\}_{n\in\mathbb{Z}}$, we define the ℓ^p norm with $p > 0$ by

$$\|a\|_{\ell^p} = \left(\sum_{n\in\mathbb{Z}} |a_n|^p\right)^{1/p}.$$

In the limit $p \to \infty$, the ℓ^∞ norm becomes the supremum norm $\|a\|_{\ell^\infty} = \sup_{n\in\mathbb{Z}} |a_n|$.

2. Derivation of the $\mathcal{PT}$-symmetric dNLS model

We consider a chain of coupled pendula displayed on Fig. 1, where each pendulum is connected to the nearest neighbors in the longitudinal and transverse directions. Newton's equations of motion are given by

$$\begin{cases} \ddot{x}_n + \sin(x_n) = C\,(x_{n+1} - 2x_n + x_{n-1}) + D(y_n - x_n), \\ \ddot{y}_n + \sin(y_n) = C\,(y_{n+1} - 2y_n + y_{n-1}) + D(x_n - y_n), \\ n \in \mathbb{Z}, \quad t \in \mathbb{R}, \end{cases} \tag{1}$$

where (x_n, y_n) correspond to the angles in each pair of the two pendula, dots denote derivatives with respect to time t, and the positive parameters C and D describe couplings between the nearest pendula in the longitudinal and transverse directions, respectively. Newton's equations (1) are related to the energy function

$$\begin{aligned} E(x,y) = \sum_{n\in\mathbb{Z}} & \frac{1}{2}(\dot{x}_n^2 + \dot{y}_n^2) + 2 - \cos(x_n) - \cos(y_n) \\ & + \frac{1}{2}C(x_{n+1} - x_n)^2 + \frac{1}{2}C(y_{n+1} - y_n)^2 \\ & + \frac{1}{2}D(x_n - y_n)^2. \end{aligned} \tag{2}$$

Dynamics of coupled pendula is considered under the following simplifying assumptions:

(A1) The coupling parameters C and D are small.
(A2) A uniform periodic force is applied to the common strings for each pair of coupled pendula and the frequency of the periodic force is picked at the $1:2$ resonance with the linear frequency of each pendulum.

According to (A1), we introduce a small parameter μ such that both C and D are proportional to μ^2. According to (A2), we consider D to be proportional to $\cos(2\omega t)$, where $|\omega - 1|$ is proportional to μ^2. We denote the proportionality coefficients by ϵ, γ, and Ω, respectively, hence parameters C and D are given by

$$C = \epsilon\mu^2, \quad D(t) = 2\gamma\mu^2\cos(2\omega t), \quad \omega^2 = 1 + \mu^2\Omega, \tag{3}$$

where γ, ϵ, Ω are μ-independent parameters. In the formal limit $\mu \to 0$, the pendula are uncoupled, and their small-amplitude oscillations can be studied with the asymptotic multi-scale expansion

$$\begin{cases} x_n(t) = \mu\left[A_n(\mu^2 t)e^{i\omega t} + \bar{A}_n(\mu^2 t)e^{-i\omega t}\right] + \mu^3 X_n(t;\mu), \\ y_n(t) = \mu\left[B_n(\mu^2 t)e^{i\omega t} + \bar{B}_n(\mu^2 t)e^{-i\omega t}\right] + \mu^3 Y_n(t;\mu), \end{cases} \tag{4}$$

where (A_n, B_n) are amplitudes for nearly harmonic oscillations and (X_n, Y_n) are remainder terms. Rigorous justification of the asymptotic expansions (4) in a similar context has been developed in [14], see also [4,8] for similar expansions.

From the conditions that the remainder terms (X_n, Y_n) remain bounded as the system evolves, it can be shown by straightforward computations that the amplitudes (A_n, B_n) satisfy the discrete nonlinear Schrödinger (dNLS) equations in the following form:

$$\begin{cases} i\frac{dA_n}{d\tau} = \epsilon\,(A_{n+1} - 2A_n + A_{n-1}) + \Omega A_n \\ \qquad\quad + \gamma(\bar{B}_n - \bar{A}_n) + \frac{1}{2}|A_n|^2 A_n, \\ i\frac{dB_n}{d\tau} = \epsilon\,(B_{n+1} - 2B_n + B_{n-1}) + \Omega B_n \\ \qquad\quad + \gamma(\bar{A}_n - \bar{B}_n) + \frac{1}{2}|B_n|^2 B_n, \end{cases} \quad n \in \mathbb{Z}, \tag{5}$$

where $\tau = \frac{1}{2}\mu^2 t$. The system (5) takes the form of coupled parametrically driven dNLS equations. There exists an invariant reduction of system (5) to the scalar dNLS equation [11] if

$$A_n = B_n, \quad n \in \mathbb{Z}. \tag{6}$$

The reduction (6) corresponds to the synchronization in each pair of coupled pendula with

$$x_n = y_n, \quad n \in \mathbb{Z}, \tag{7}$$

when the periodic driving force does not affect the dynamics of the coupled pendula chain.

Unless the reduction (6) is imposed, the system of coupled dNLS equations (5) is not invariant with respect to transformation of the phases of (A, B). It is however invariant with respect to the exchange $A \leftrightarrow B$. The system can be written in a complex Hamiltonian form:

$$i\frac{dA_n}{d\tau} = \frac{\partial H}{\partial \bar{A}_n}, \quad i\frac{dB_n}{d\tau} = \frac{\partial H}{\partial \bar{B}_n}, \quad n \in \mathbb{Z}, \tag{8}$$

associated with the conserved energy function

$$H(A,B)=\sum_{n\in\mathbb{Z}}\frac{1}{4}(|A_n|^4+|B_n|^4)+\Omega(|A_n|^2+|B_n|^2)+\gamma(A_nB_n+\bar{A}_n\bar{B}_n)-\frac{1}{2}\gamma(A_n^2+\overline{A}_n^2+B_n^2+\overline{B}_n^2)-\epsilon|A_{n+1}-A_n|^2-\epsilon|B_{n+1}-B_n|^2. \tag{9}$$

The Hamiltonian structure (8) and the conserved energy function (9) are inherited from the energy function (2) of the Newton's equations (1) after the substitution of the asymptotic expansion (4) and its truncation. If the coupling parameter D depends on time, the energy function $E(x,y)$ is not conserved in (2). However, the asymptotic expansion (4) simplifies equations of motion near the $1:2$ resonance so that the leading-order system (5) is now autonomous with the conserved energy function $H(A,B)$ in (9). Such simplifications of equations of motion are generally used in studies of coupled oscillators under parametric driving force, see, e.g., [1,2].

The system (5) can be cast to the form of the parity–time reversal ($\mathcal{PT}$) dNLS equations [4,8]. Using the variables

$$u_n:=\frac{1}{4}\left(A_n-i\bar{B}_n\right),\quad v_n:=\frac{1}{4}\left(A_n+i\bar{B}_n\right), \tag{10}$$

the system of coupled dNLS equations (5) becomes

$$\begin{cases} i\frac{du_n}{d\tau}=\epsilon\,(v_{n+1}-2v_n+v_{n-1})+\Omega v_n+i\gamma u_n-\gamma\bar{u}_n \\ \qquad +2\left[\left(2|u_n|^2+|v_n|^2\right)v_n+u_n^2\bar{v}_n\right], \\ i\frac{dv_n}{d\tau}=\epsilon\,(u_{n+1}-2u_n+u_{n-1})+\Omega u_n-i\gamma v_n-\gamma\bar{v}_n \\ \qquad +2\left[\left(|u_n|^2+2|v_n|^2\right)u_n+\bar{u}_nv_n^2\right], \end{cases} \tag{11}$$

which is invariant with respect to the action of the parity $\mathcal{P}$ and time-reversal $\mathcal{T}$ operators given by

$$\mathcal{P}\begin{bmatrix}u\\v\end{bmatrix}=\begin{bmatrix}v\\u\end{bmatrix},\qquad \mathcal{T}\begin{bmatrix}u(t)\\v(t)\end{bmatrix}=\begin{bmatrix}\bar{u}(-t)\\\bar{v}(-t)\end{bmatrix}. \tag{12}$$

Therefore, the system (11) can be referred to as the $\mathcal{PT}$-symmetric dNLS equation. The system (11) is still Hamiltonian with a cross-gradient Hamiltonian structure,

$$i\frac{du_n}{d\tau}=\frac{\partial\tilde{H}}{\partial\bar{v}_n},\quad i\frac{dv_n}{d\tau}=\frac{\partial\tilde{H}}{\partial\bar{u}_n},\quad n\in\mathbb{Z}, \tag{13}$$

associated with the modified energy functional

$$\tilde{H}(u,v)=\sum_{n\in\mathbb{Z}}(|u_n|^2+|v_n|^2)^2+(u_n\bar{v}_n+\bar{u}_nv_n)^2+\Omega(|u_n|^2+|v_n|^2)-\epsilon|u_{n+1}-u_n|^2-\epsilon|v_{n+1}-v_n|^2+i\gamma(u_n\bar{v}_n-\bar{u}_nv_n)-\gamma(u_nv_n+\bar{u}_n\bar{v}_n). \tag{14}$$

The Hamiltonian system (11) is not phase-invariant, so that it does not have the mass conserved quantity. We note that the breaking of the phase invariance by the parametric driving is common to many parametrically driven chains of pendula and so is the energy conservation in the reduced amplitude equations [1,2].

The previous works [8,9] explore a different version of the $\mathcal{PT}$-symmetric dNLS equation, which is related to the Newton's equation with a different coupling between x_n and y_n pendula. The $\mathcal{PT}$-symmetric dNLS equation in [8,9] has both energy and mass conservation. Cross-gradient models considered in the classification work [4] also assumed conservation of both energy and mass. In the present work, we address the $\mathcal{PT}$-symmetric dNLS equation with conserved energy but no phase-invariance. In this context, we prefer to work with the dNLS system (5) without transforming it to the $\mathcal{PT}$-symmetric dNLS equation (11).

3. Linear stability of zero equilibrium

Parametrically driving forces can destabilize the zero equilibrium state in the coupled pendula chain. We shall first clarify conditions for the linear stability of the zero equilibrium. The following lemma provides a sharp bound on the parameter γ of the driving force which ensures that the zero equilibrium is linearly stable.

Lemma 1. *The zero equilibrium of the system (5) with $\epsilon>0$ is linearly stable if $|\gamma|<\gamma_0$, where*

$$\gamma_0:=\begin{cases}\frac{1}{2}(\Omega-4\epsilon), & \Omega>4\epsilon,\\ \frac{1}{2}|\Omega|, & \Omega<0.\end{cases} \tag{15}$$

The zero equilibrium is linearly unstable if $|\gamma|\geq\gamma_0$ or if $\Omega\in[0,4\epsilon]$ and $\gamma\neq0$.

Proof. Truncating the system (5) at the linear terms and using the Fourier transform

$$A_n=\frac{1}{2\pi}\int_{-\pi}^{\pi}\hat{A}e^{in\theta}d\theta,\quad n\in\mathbb{Z}, \tag{16}$$

we obtain the following system of differential equations for $\hat{A}$ and $\hat{B}$ parameterized by θ:

$$\begin{cases} i\frac{d\hat{A}}{d\tau}+\kappa\hat{A}=\gamma(\hat{\bar{B}}-\hat{\bar{A}}), \\ i\frac{d\hat{B}}{d\tau}+\kappa\hat{B}=\gamma(\hat{\bar{A}}-\hat{\bar{B}}), \end{cases} \tag{17}$$

where $\kappa:=4\epsilon\sin^2(\theta/2)-\Omega$. Separating the time variable like in $\hat{A}(\tau)=\hat{a}e^{i\omega\tau}$ yields the linear homogeneous system

$$\begin{bmatrix}\kappa-\omega & \gamma & 0 & -\gamma\\ \gamma & \kappa+\omega & -\gamma & 0\\ 0 & -\gamma & \kappa-\omega & \gamma\\ -\gamma & 0 & \gamma & \kappa+\omega\end{bmatrix}\begin{bmatrix}\hat{a}\\\hat{\bar{a}}\\\hat{b}\\\hat{\bar{b}}\end{bmatrix}=\begin{bmatrix}0\\0\\0\\0\end{bmatrix},$$

with the characteristic equation factorized in the form

$$(\omega^2-\kappa^2)(\omega^2-\kappa^2+4\gamma^2)=0. \tag{18}$$

The first pair of roots is always real:

$$\omega_1^{\pm}=\pm|\kappa|=\pm\left|4\epsilon\sin^2(\theta/2)-\Omega\right|.$$

The second pair of roots is real if $|\kappa|>2|\gamma|$:

$$\omega_2^{\pm}=\pm\sqrt{\kappa^2-4\gamma^2}=\pm\sqrt{(4\epsilon\sin^2(\theta/2)-\Omega)^2-4\gamma^2}.$$

This happens for $2|\gamma|<\Omega-4\epsilon$ if $\Omega>4\epsilon$ and for $2|\gamma|<|\Omega|$ if $\Omega<0$. In both cases, the zero equilibrium is linearly stable.

On the other hand, for any $|\gamma|>\gamma_0$, the values of $\omega_2^{\pm}$ are purely imaginary either near $\theta=\pm\pi$ if $\Omega>4\epsilon$ or near $\theta=0$ if $\Omega<0$. In these cases, the zero equilibrium is linearly unstable with exponentially growing perturbations. For $|\gamma|=\gamma_0$, the values of $\omega_2^{\pm}$ are zero either at $\theta=\pm\pi$ if $\Omega>4\epsilon$ or at $\theta=0$ if $\Omega<0$. The zero equilibrium is linearly unstable with polynomially growing perturbations.

Finally, if $\Omega\in[0,4\epsilon]$, there exists $\theta_0\in[-\pi,\pi]$ such that $\kappa=0$. Then, for any $\gamma\neq0$, the values of $\omega_2^{\pm}$ are purely imaginary and the zero equilibrium is linearly unstable with exponentially growing perturbations. □

4. Nonlinear stability of coupled pendula

The Cauchy problem for the system of coupled dNLS equations (5) can be posed in sequence space $\ell^2(\mathbb{Z})$. Local existence of solutions to the Cauchy problem in $\ell^2(\mathbb{Z})$ follows from an easy application of Picard's method. Combining local existence with energy estimates yields global existence of solutions. The following lemma states the global well-posedness result.

Lemma 2. *For every $(A^{(0)}, B^{(0)}) \in \ell^2(\mathbb{Z})$, there exists a unique solution $(A, B)(\tau) \in C^1(\mathbb{R}, \ell^2(\mathbb{Z}))$ of the system of coupled dNLS equations (5) such that $(A, B)(0) = (A^{(0)}, B^{(0)})$. The unique solution depends continuously on initial data $(A^{(0)}, B^{(0)}) \in \ell^2(\mathbb{Z})$.*

Proof. The Cauchy problem for the system of coupled dNLS equations (5) can be posed by using the system of integral equations

$$\begin{cases} A(\tau) = A^{(0)} - i\int_0^\tau F_A(A(\tau'), B(\tau'))d\tau', \\ B(\tau) = B^{(0)} - i\int_0^\tau F_B(A(\tau'), B(\tau'))d\tau', \end{cases} \tag{19}$$

where (F_A, F_B) stand for the right-hand sides of the system (5). Since the discrete Laplacian is a bounded operator in $\ell^2(\mathbb{Z})$ with the bound

$$\sum_{n\in\mathbb{Z}} |A_{n+1} - A_n|^2 \le 4\|A\|_{\ell^2}^2, \quad A \in \ell^2(\mathbb{Z}), \tag{20}$$

and the sequence space $\ell^2(\mathbb{Z})$ forms a Banach algebra with respect to pointwise multiplication with the bound

$$\|AB\|_{\ell^2} \le \|A\|_{\ell^2}\|B\|_{\ell^2}, \quad A, B \in \ell^2(\mathbb{Z}), \tag{21}$$

there is a sufficiently small $\tau_0 > 0$ such that the integral equations (19) admit a unique solution $(A, B)(\tau) \in C^0([-\tau_0, \tau_0], \ell^2(\mathbb{Z}))$ with $(A, B)(0) = (A^{(0)}, B^{(0)})$. This follows by the contraction mapping method, which also ensures that the solution depends continuously on initial data $(A^{(0)}, B^{(0)}) \in \ell^2(\mathbb{Z})$. Thanks again to the boundedness of the discrete Laplacian operator in $\ell^2(\mathbb{Z})$, bootstrap arguments extend this solution in $C^1([-\tau_0, \tau_0], \ell^2(\mathbb{Z}))$.

The local solution is continued globally by using the energy method. The following balance equation is obtained from system (5) for any solution $(A, B)(\tau)$ in $C^1([-\tau_0, \tau_0], \ell^2(\mathbb{Z}))$:

$$\frac{d}{d\tau}\sum_{n\in\mathbb{Z}}(|A_n|^2 + |B_n|^2) = i\gamma\sum_{n\in\mathbb{Z}}\left(2A_nB_n - 2\bar{A}_n\bar{B}_n + \bar{A}_n^2 + \bar{B}_n^2 - A_n^2 - B_n^2\right).$$

By integrating this equation in time and estimating the integral with the triangle inequality, we obtain

$$\|A(\tau)\|_{l^2}^2 + \|B(\tau)\|_{l^2}^2 \le \left(\|A^{(0)}\|_{l^2}^2 + \|B^{(0)}\|_{l^2}^2\right) + 4|\gamma|\int_0^{|\tau|}\left(\|A(\tau')\|_{l^2}^2 + \|B(\tau')\|_{l^2}^2\right)d\tau'.$$

Gronwall's inequality yields

$$\|A(\tau)\|_{l^2}^2 + \|B(\tau)\|_{l^2}^2 \le \left(\|A^{(0)}\|_{l^2}^2 + \|B^{(0)}\|_{l^2}^2\right)e^{4|\gamma\tau|}, \quad \tau \in [-\tau_0, \tau_0]. \tag{22}$$

Therefore $\|A(\tau)\|_{l^2}$ and $\|B(\tau)\|_{l^2}$ cannot blow up in a finite time and so cannot their derivatives in τ. Therefore, the local solution $(A, B)(\tau) \in C^1([-\tau_0, \tau_0], \ell^2(\mathbb{Z}))$ is continued for every τ_0. □

The bound (22) does not exclude a possible exponential growth of the $\ell^2(\mathbb{Z})$ norms of the global solution $(A, B)(\tau)$ as $\tau \to \infty$. However, thanks to coercivity of the energy function (9) near the zero equilibrium, we can still obtain a time-independent bound on the $\ell^2(\mathbb{Z})$ norm of the solution near the zero equilibrium, provided it is linearly stable. Moreover, for $\Omega > (2|\gamma| + 4\epsilon)$, the global bound holds for arbitrary initial data. The following three theorems represent the corresponding results. For simplicity, we can restrict our attention to $\gamma > 0$.

Theorem 1. *For every $\Omega > 2\gamma + 4\epsilon$ and every initial data $(A^{(0)}, B^{(0)}) \in \ell^2(\mathbb{Z})$, there is a positive constant C such that the unique solution $(A, B)(\tau) \in C^1(\mathbb{R}, \ell^2(\mathbb{Z}))$ of the system of coupled dNLS equations (5) satisfies*

$$\|A(\tau)\|_{\ell^2}^2 + \|B(\tau)\|_{\ell^2}^2 \le C, \quad \text{for every } \tau \in \mathbb{R}. \tag{23}$$

Proof. If $\Omega > 2\gamma + 4\epsilon$, the following lower bound for the energy function H is positive:

$$H \ge (\Omega - 2\gamma - 4\epsilon)\left(\|A(\tau)\|_{\ell^2}^2 + \|B(\tau)\|_{\ell^2}^2\right), \quad \tau \in \mathbb{R}, \tag{24}$$

where we have used the Cauchy–Schwarz inequality and the bound (20) and we have dropped the positive quartic terms from the lower bound. Since H is constant in τ and is bounded for any $(A, B)(\tau) \in C^1(\mathbb{R}, \ell^2(\mathbb{Z}))$ due to the continuous embedding

$$\|A\|_{\ell^4} \le \|A\|_{\ell^2}, \quad A \in \ell^2(\mathbb{Z}), \tag{25}$$

the time-independent bound (23) follows from the lower bound (24) for any $\Omega > 2\gamma + 4\epsilon$. □

Theorem 2. *For every $\Omega < -2\gamma$, there exist $\delta_0 > 0$ and $C_0 > 0$ such that for every initial data $(A^{(0)}, B^{(0)}) \in \ell^2(\mathbb{Z})$ satisfying*

$$\delta := \|A^{(0)}\|_{\ell^2}^2 + \|B^{(0)}\|_{\ell^2}^2 \le \delta_0, \tag{26}$$

the unique solution $(A, B)(\tau) \in C^1(\mathbb{R}, \ell^2(\mathbb{Z}))$ of the system of coupled dNLS equations (5) satisfies

$$\|A(\tau)\|_{\ell^2}^2 + \|B(\tau)\|_{\ell^2}^2 \le C_0\delta, \quad \text{for every } \tau \in \mathbb{R}. \tag{27}$$

Proof. If $\Omega < -2\gamma$, the following lower bound for the energy function $-H$ holds:

$$-H \ge (|\Omega| - 2\gamma)\left(\|A(\tau)\|_{\ell^2}^2 + \|B(\tau)\|_{\ell^2}^2\right) - \frac{1}{4}\left(\|A(\tau)\|_{\ell^2}^2 + \|B(\tau)\|_{\ell^2}^2\right)^2, \quad \tau \in \mathbb{R}, \tag{28}$$

where we have used the Cauchy–Schwarz inequality and the bound (25) and we have dropped the positive discrete Laplacian terms from the lower bound. Since $-H > 0$ is constant in τ and the initial data in (26) is small, there exists a constant $C > 0$ independently of δ, such that $|H| \le C\delta$. The lower bound (28) yields the upper bound (27) with the choice of constant $C_0 > 0$ to satisfy

$$\frac{C\delta}{|\Omega| - 2\gamma - \frac{1}{4}C_0\delta} \le C_0\delta. \tag{29}$$

It is always possible to satisfy the inequality (29) since C and C_0 are δ-independent and $\delta \le \delta_0$ with sufficiently small δ_0. □

Theorem 3. *If the lattice is truncated on finitely many (N) sites, denoted by $\mathbb{Z}_N$, then for every Ω, γ, ϵ and every initial data $(A^{(0)}, B^{(0)}) \in \ell^2(\mathbb{Z}_N)$, there is a positive constant C_N such that the unique solution $(A, B)(\tau) \in C^1(\mathbb{R}, \ell^2(\mathbb{Z}_N))$ of the system of coupled dNLS equations (5) on the truncated lattice $\mathbb{Z}_N$ satisfies*

$$\|A(\tau)\|_{\ell^2}^2 + \|B(\tau)\|_{\ell^2}^2 \le C_N, \quad \text{for every } \tau \in \mathbb{R}, \tag{30}$$

with $C_N \to \infty$ as $N \to \infty$.

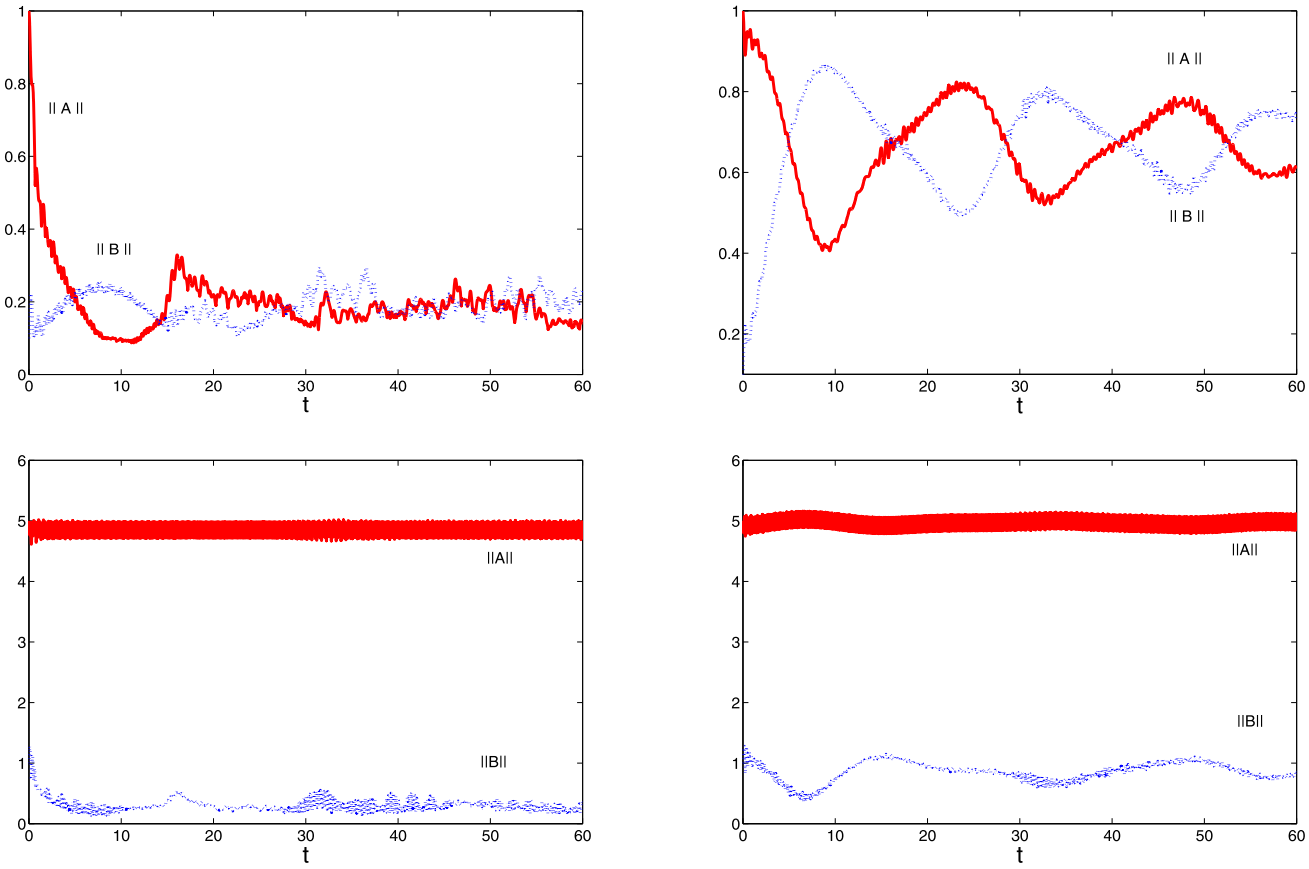

Fig. 2. ℓ^∞ (left) and ℓ^2 (right) norms of the solution for A (red solid) and B (blue dotted) for $\Omega = 8$: upper panels for $(A_0, B_0) = (1, 0.1)$ and lower panels for $(A_0, B_0) = (5, 1)$. (For interpretation of the references to color in this figure legend, the reader is referred to the web version of this article.)

Proof. If the lattice is truncated on N sites, one can use the bound

$$\|A\|_{\ell^2} \leq N^{1/4} \|A\|_{\ell^4}, \quad A \in \ell^4(\mathbb{Z}_N), \tag{31}$$

and obtain a different lower bound for the energy function H:

$$H \geq \frac{1}{4}\left(\|A(\tau)\|_{\ell^4}^4 + \|B(\tau)\|_{\ell^4}^4\right) - (|\Omega| + \gamma + 4\epsilon) N^{1/2} \left(\|A(\tau)\|_{\ell^4}^2 + \|B(\tau)\|_{\ell^4}^2\right), \quad \tau \in \mathbb{R}.$$

Since H is constant in τ, the time-independent bound (30) follows from the lower bound above with $C_N < \infty$. However, $C_N \to \infty$ as $N \to \infty$. □

5. Numerical experiments

We present here numerical approximations of dynamics of the dNLS system (5). For simplicity, all simulations correspond to the choice $\gamma = 1$ and $\epsilon = 1$. The lattice is truncated on N sites with an odd choice for N. The resulting finite system of differential equations is approximated by the MATLAB solver *ode45* with relative tolerance set at 10^{-7} and absolute tolerance set at 10^{-9}.

Figs. 2–6 show the dependence of the ℓ^∞ (left) and ℓ^2 (right) norms of the components A (red solid) and B (blue dotted) in the chain of $N = 61$ pendula for three characteristic values of the parameter Ω.

For $\Omega = 8 > 2\gamma + 4\epsilon$, the result of Theorem 1 provides a global bound on the $\ell^2(\mathbb{Z})$ norm of the solution. This is confirmed by the numerical simulation on Figs. 2 and 3. The upper panels show computations for the initial data which are nonzero on the central site with $(A_0, B_0) = (1, 0.1)$. The lower panels show computations with $(A_0, B_0) = (5, 1)$. As a measure of the numerical error, we control conservation of energy H in (9). We have observed that the energy is conserved up to the order of 10^{-6} for smaller initial data (upper panels) and up to the order of 10^{-4} for larger initial data (lower panels).

On Figs. 2 and 3, the upper panels show that for smaller initial conditions, the central pendulum excites other pendula in the chain, this process results in the decrease of the oscillation amplitude of the central pendulum. While the ℓ^2 norm oscillates between the modes A and B, the ℓ^∞ norms of both modes A and B are comparable and do not change much in the time evolution after an initial time interval. The lower panels show that for larger initial conditions, dynamics of the A mode is effectively separated from dynamics of the B modes and the central pendulum does not excite large oscillations of other pendula.

For $\Omega = -4 < -2\gamma$, the result of Theorem 2 provides a global bound on the $\ell^2(\mathbb{Z})$ norm of the solution only in the case of small initial conditions. On Figs. 4 and 5, the numerical simulations on the upper panels for smaller initial conditions do not show drastic differences compared to the case $\Omega = 8 > 2\gamma + 4\epsilon$. The lower panels for larger initial conditions show that the A and B modes mix up and that the central pendulum excites large oscillations of other pendula in the chain. As a result, the ℓ^2 norm of the solution grows whereas the ℓ^∞ norm stays at the same level as the initial data.

For $\Omega = 0 \in (-2\gamma, 2\gamma + 4\epsilon)$, the result of Lemma 1 implies the linear instability of the zero equilibrium. Since the energy methods are not useful to control global dynamics of large solutions far from the zero equilibrium, the numerical simulations give us the way to explore this phenomenon. Numerical simulation on Fig. 6 shows that the growth of oscillation amplitudes stabilizes

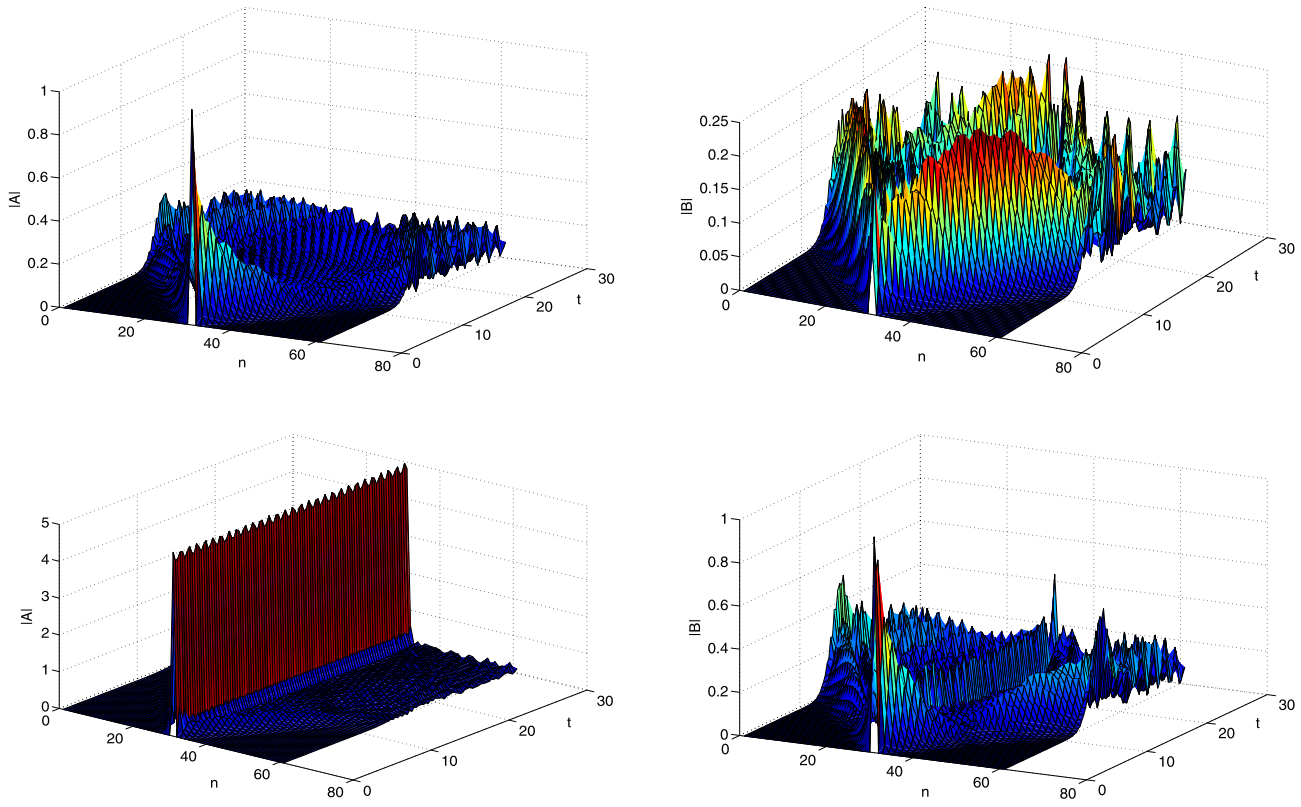

Fig. 3. Surface plots for $|A|$ (left) and $|B|$ (right) for $\Omega = 8$: upper panels for $(A_0, B_0) = (1, 0.1)$ and lower panels for $(A_0, B_0) = (5, 1)$. (For interpretation of the colors in this figure, the reader is referred to the web version of this article.)

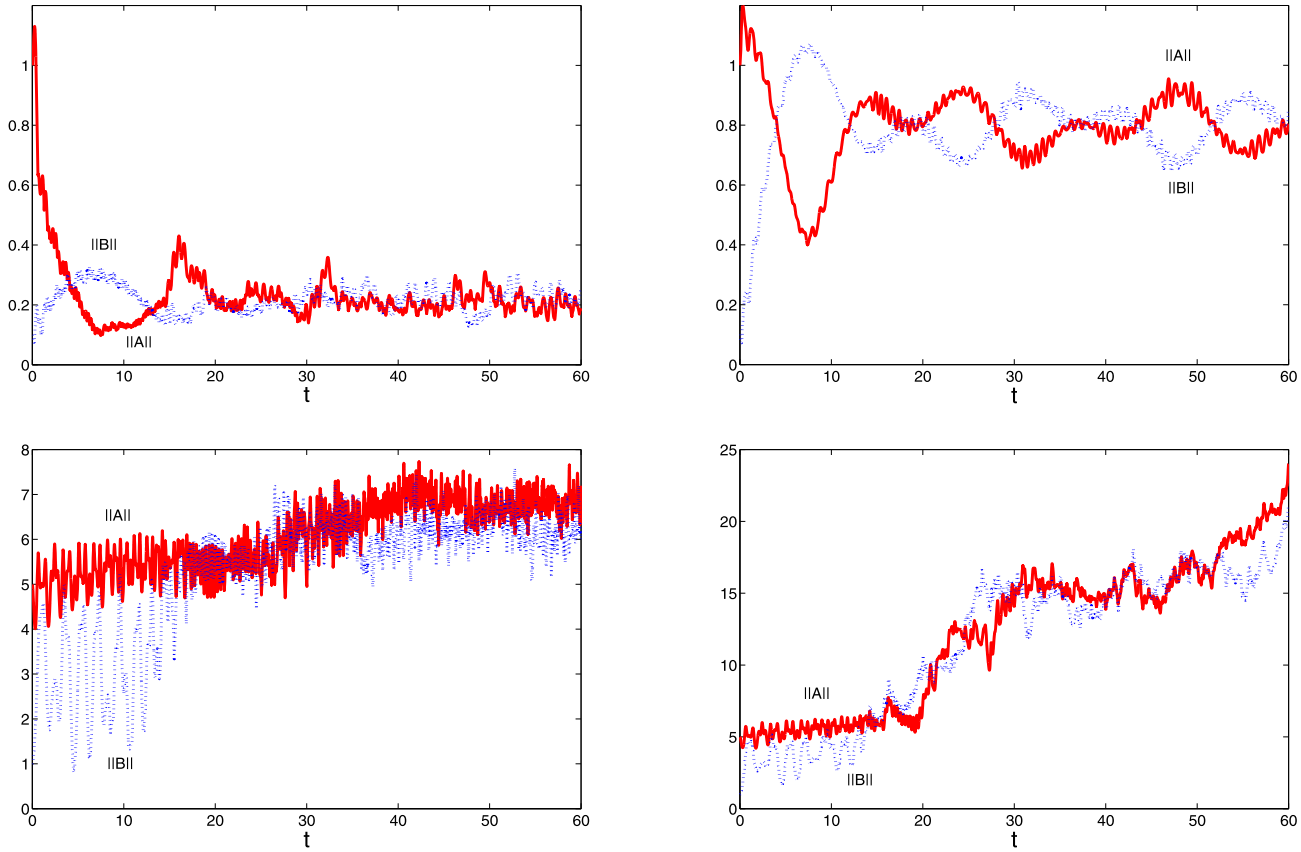

Fig. 4. ℓ^∞ (left) and ℓ^2 (right) norms of the solution for A (red solid) and B (blue dotted) for $\Omega = -4$: upper panels for $(A_0, B_0) = (1, 0.1)$ and lower panels for $(A_0, B_0) = (5, 1)$. (For interpretation of the references to color in this figure legend, the reader is referred to the web version of this article.)

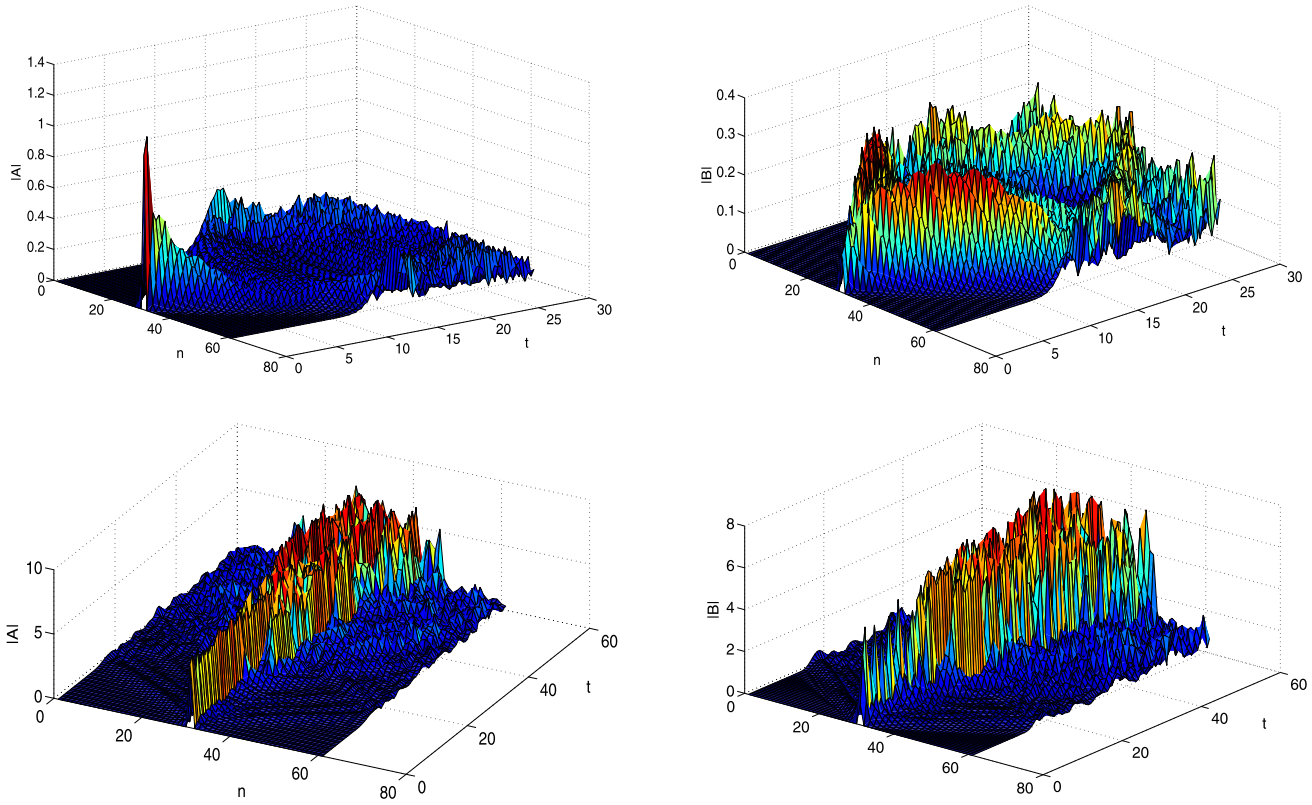

Fig. 5. Surface plots for $|A|$ (left) and $|B|$ (right) for $\Omega = -4$: upper panels for $(A_0, B_0) = (1, 0.1)$ and lower panels for $(A_0, B_0) = (5, 1)$. (For interpretation of the colors in this figure, the reader is referred to the web version of this article.)

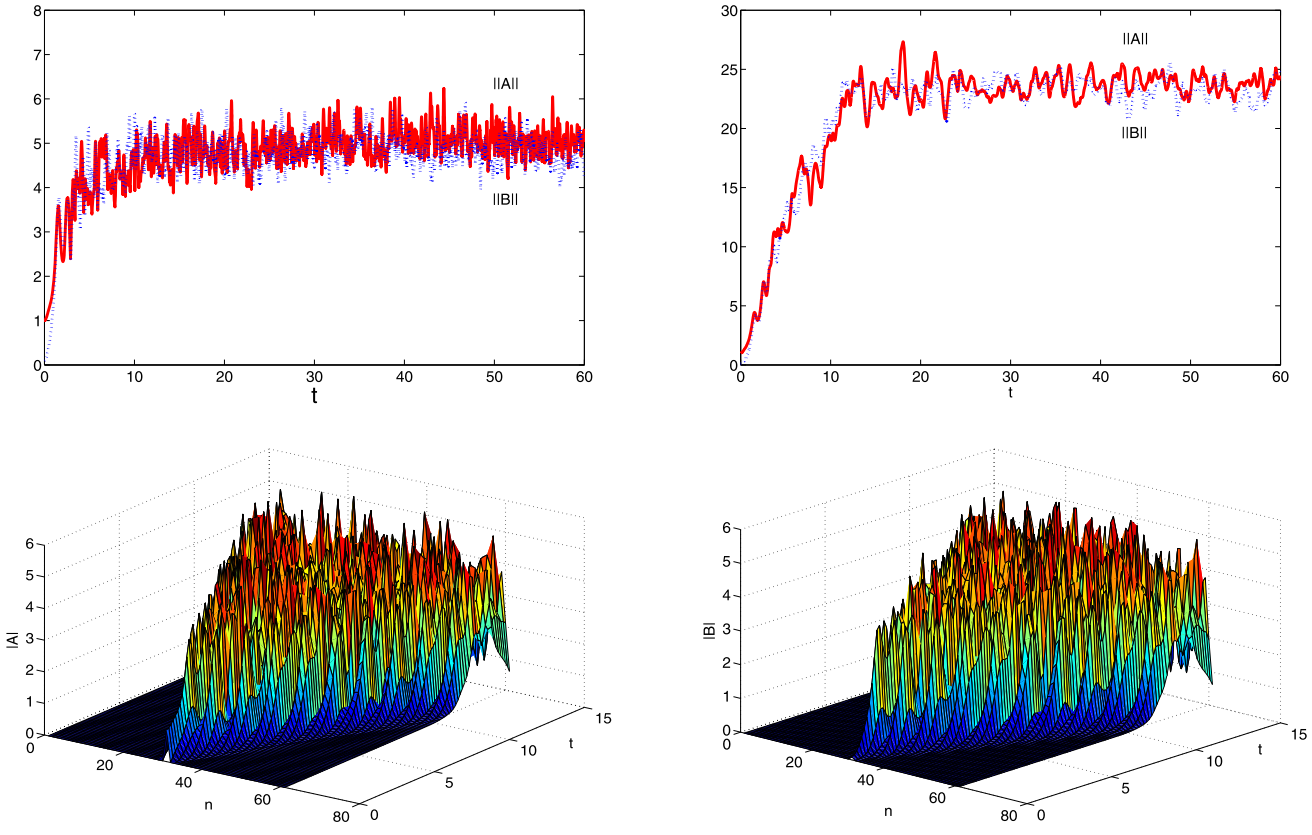

Fig. 6. Upper panels: ℓ^∞ (left) and ℓ^2 (right) norms of the solution for A (red solid) and B (blue dotted) for $\Omega = 0$ and $(A_0, B_0) = (1, 0.1)$. Lower panels: surface plots for $|A|$ (left) and $|B|$ (right). (For interpretation of the references to color in this figure legend, the reader is referred to the web version of this article.)

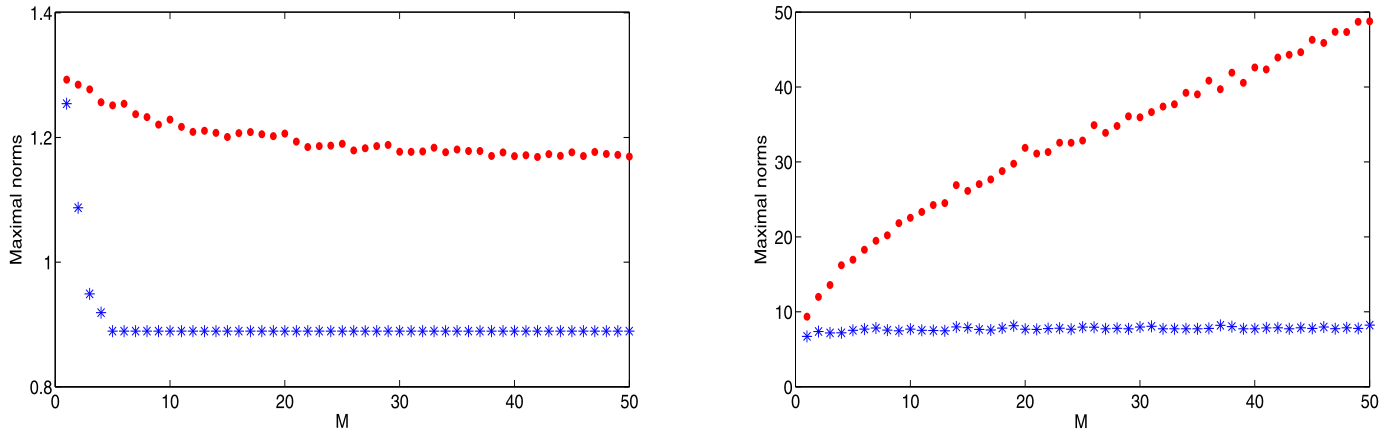

Fig. 7. Dependence of the maximal ℓ^2 norm (red dots) and the ℓ^∞ norm (blue stars) of the solution on the time interval $[10, 70]$ versus M, where $N = 2M + 1$ is the number of oscillators, for $\Omega = -4$ (left) and $\Omega = 0$ (right), in the case $(A_0, B_0) = (1, 0.1)$. (For interpretation of the references to color in this figure legend, the reader is referred to the web version of this article.)

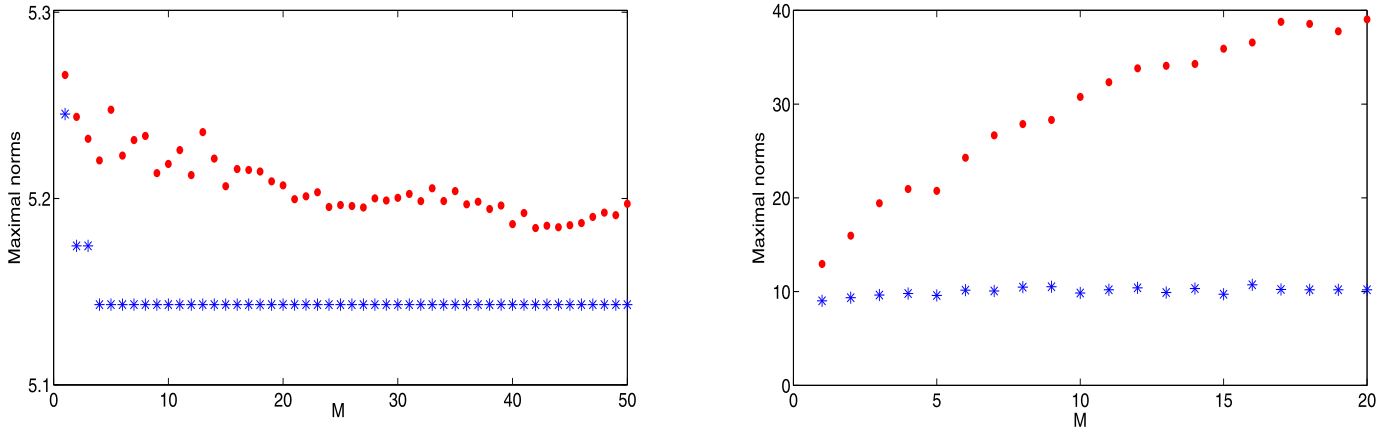

Fig. 8. The same as Fig. 7 but for $\Omega = 8$ (left) and $\Omega = -4$ (right), in the case $(A_0, B_0) = (5, 1)$.

at a certain level of the ℓ^∞ norm and that the ℓ^2 norm of the solution is significantly larger than the ℓ^∞ norm. This indicates that many pendula are excited and oscillate with large and comparable amplitudes with respect to the central pendulum. Very similar patterns were observed for larger initial amplitude of the central pendulum (not shown).

By Theorem 3, the solution in the finite chain of N oscillators cannot grow without bounds as $t \to \infty$. At the same time, the growth of the ℓ^2 norm of the solution as $t \to \infty$ is not ruled out for the unbounded lattice in the case $\Omega < 2\gamma + 4\epsilon$. In order to illustrate that this growth does occur, we run numerical experiments, in which we compute the maximal ℓ^2 norm of the solution on the time interval $[10, 70]$ versus M, where $N = 2M + 1$ is the number of sites. Fig. 7 (right) shows the nearly monotonic growth of the ℓ^2 norm (red dots) of the solution in M in the case $\Omega = 0 \in (-2\gamma, 2\gamma + 4\epsilon)$, confirming our conjecture on the growth of the solution in the unbounded lattice as $t \to \infty$. The ℓ^∞ norm (blue stars) of the solution saturates to the same level independently of M.

Fig. 7 (left) shows a similar computation for $\Omega = -4 < -2\gamma$ starting with the smaller initial condition $(A_0, B_0) = (1, 0.1)$. In this case, the ℓ^2 norm of the solution decreases in M and approaches to a certain limiting level. This indicates that the growth of the solution on the unbounded lattice does not occur for $\Omega < -2\gamma$ in the case of smaller initial amplitude, in agreement with Theorem 2. Similar dependence (not shown) exists for $\Omega = 8 > 2\gamma + 4\epsilon$, when the energy method excludes growth of the large-norm solutions (see Theorem 1).

Similar simulations were carried for initial data with larger amplitudes $(A_0, B_0) = (5, 1)$ and they are shown on Fig. 8 for $\Omega = 8$ (left) and $\Omega = -4$ (right). The maximal ℓ^2 norm does not change versus the number of oscillators N in the case $\Omega = 8 > 2\gamma + 4\epsilon$, in agreement with Theorem 1. At the same time, the maximal ℓ^2 norm grows with M (and N) for $\Omega = -4 < -2\gamma$ and apparently diverges as $N \to \infty$. This experiment implies that the limitation of Theorem 2 for small initial data is not a technical shortfall, the solution (A, B) can grow as $t \to \infty$ in the unbounded lattice in the case $\Omega < -2\gamma$.

We note that another numerical solver was also used to approximate dynamics of the dNLS system (5). The alternative solver combines a Crank–Nicolson scheme with the fixed-point iteration method to solve the coupled system of differential equations and it was implemented in Python and Fortran. The numerical experiments shown on Figs. 2–8 were reproduced on this other solver without any significant differences.

6. Conclusion

We have addressed a novel model of the $\mathcal{PT}$-symmetric dNLS equation, which admits Hamiltonian formulation but exhibits no phase invariance. The model describes dynamics in the chain of weakly coupled pendula pairs near the $1:2$ resonance between the parametrically driven force and the linear frequency of each pendulum.

In the context of the problem of nonlinear stability of zero equilibrium, we have obtained sharp bounds on the ℓ^2 norms of the

oscillation amplitudes in terms of parameters of the model and the size of the initial condition. Stable dynamics of the coupled pendula chains is relatively simple, but it becomes more interesting when the stability constraints are not satisfied. In the latter cases, we show that the central pendulum excites nearest pendula such that the ℓ^2 norm of the oscillation amplitudes grows while the ℓ^∞ norm remains finite.

For future work, it may be interesting to characterize breathers (periodic or quasi-periodic solutions) of the model and to see how existence and stability of such solutions is related to the nonlinear stability of the zero equilibrium. Another open question is to address stable and unstable dynamics in the original Newton's equations for coupled pendula and to compare it with predictions of the reduced dNLS model.

Acknowledgements

D.E. Pelinovsky thanks members of LAMIA at Université des Antilles for hospitality during his visit in May 2017. The authors thank A. Chernyavsky for preparing Fig. 1. The results of this work were obtained with the financial support from the state task of Russian Federation in the sphere of scientific activity (Task No. 5.5176.2017/8.9).

References

[1] N.V. Alexeeva, I.V. Barashenkov, G.P. Tsironis, Impurity-induced stabilization of solitons in arrays of parametrically driven nonlinear oscillators, Phys. Rev. Lett. 84 (2000) 3053–3056.
[2] I.V. Barashenkov, N.V. Alexeeva, E.V. Zemlyanaya, Two- and three-dimensional oscillons in nonlinear Faraday resonance, Phys. Rev. Lett. 89 (2002) 104101.
[3] I.V. Barashenkov, M. Gianfreda, An exactly solvable PT-symmetric dimer from a Hamiltonian system of nonlinear oscillators with gain and loss, J. Phys. A, Math. Theor. 47 (2014) 282001.
[4] I.V. Barashenkov, D.E. Pelinovsky, P. Dubard, Dimer with gain and loss: integrability and $\mathcal{PT}$-symmetry restoration, J. Phys. A, Math. Theor. 48 (2015) 325201.
[5] C.M. Bender, Making sense of non-Hermitian Hamiltonians, Rep. Prog. Phys. 70 (2007) 947.
[6] C.M. Bender, B. Berntson, D. Parker, E. Samuel, Observation of PT phase transition in a simple mechanical system, Am. J. Phys. 81 (2013) 173.
[7] O.M. Braun, Y. Kivshar, The Frenkel–Kontorova Model: Concepts, Methods, and Applications, Springer-Verlag, Berlin, Heidelberg, 2004.
[8] A. Chernyavsky, D.E. Pelinovsky, Breathers in Hamiltonian $\mathcal{PT}$-symmetric chains of coupled pendula under a resonant periodic force, Symmetry 8 (2016) 59.
[9] A. Chernyavsky, D.E. Pelinovsky, Long-time stability of breathers in Hamiltonian $\mathcal{PT}$-symmetric lattices, J. Phys. A 49 (2016) 475201.
[10] J. Cuevas, L.Q. English, P.G. Kevrekidis, M. Anderson, Discrete breathers in a forced-damped array of coupled pendula: modeling, computation, and experiment, Phys. Rev. Lett. 102 (2009) 224101.
[11] P.G. Kevrekidis, The Discrete Nonlinear Schrödinger Equation, Springer-Verlag, Berlin, Heidelberg, 2009.
[12] P.G. Kevrekidis, D.E. Pelinovsky, D.Y. Tyugin, Nonlinear dynamics in PT-symmetric lattices, J. Phys. A, Math. Theor. 46 (2013) 365201.
[13] F. Palmero, J. Han, L.Q. English, T.J. Alexander, P.G. Kevrekidis, Multifrequency and edge breathers in the discrete sine–Gordon system via subharmonic driving: theory, computation and experiment, Phys. Lett. A 380 (2016) 402–407.
[14] D. Pelinovsky, T. Penati, S. Paleari, Approximation of small-amplitude weakly coupled oscillators with discrete nonlinear Schrödinger equations, Rev. Math. Phys. 28 (2016) 1650015.
[15] D.E. Pelinovsky, D.A. Zezyulin, V.V. Konotop, Nonlinear modes in a generalized $\mathcal{PT}$-symmetric discrete nonlinear Schrodinger equation, J. Phys. A, Math. Theor. 47 (2014) 085204.
[16] D.E. Pelinovsky, D.A. Zezyulin, V.V. Konotop, Global existence of solutions to coupled $\mathcal{PT}$-symmetric nonlinear Schrödinger equations, Int. J. Theor. Phys. 54 (2015) 3920–3931.
[17] A. Pikovsky, M. Rosenblum, J. Kurths, Synchronization: A Universal Concept in Nonlinear Sciences, Cambridge Nonlinear Science Series, vol. 12, Cambridge University Press, Cambridge, 2003.
[18] E. Destyl, S.P. Nuiro, P. Poullet, On the global behavior of solutions of a coupled system of nonlinear Schrödinger equation, Stud. Appl. Math. 138 (2017) 227–244.
[19] J. Schindler, A. Li, M.C. Zheng, F.M. Ellis, T. Kottos, Experimental study of active LRC circuits with PT symmetries, Phys. Rev. A 84 (2011) 040101.
[20] H. Susanto, Q.E. Hoq, P.G. Kevrekidis, Stability of discrete solitons in the presence of parametric driving, Phys. Rev. E 74 (2006) 067601.
[21] M. Syafwan, H. Susanto, S.M. Cox, Discrete solitons in electromechanical resonators, Phys. Rev. E 81 (2010) 026207.
[22] Y. Xu, T.J. Alexander, H. Sidhu, P.G. Kevrekidis, Instability dynamics and breather formation in a horizontally shaken pendulum chain, Phys. Rev. E 90 (2014) 042921.